THE JOURNAL OF BIOLOGICAL CHEMISTRY VOL. 287, NO. 15, pp. 12395–12404, April 6, 2012

Endotoxin Priming of Neutrophils Requires Endocytosis and NADPH Oxidase-dependent Endosomal Reactive Oxygen Species*

Received for publication, September 21, 2011, and in revised form, December 13, 2011 Published, JBC Papers in Press, January 10, 2012, DOI 10.1074/jbc.M111.306530

Fred S. Lamb[‡], Jessica S. Hook[‡§], Brieanna M. Hilkin[‡§], Jody N. Huber[‡§], A. Paige Davis Volk[‡§], and Jessica G. Moreland[‡§1]

From the [‡]Division of Critical Care, Department of Pediatrics and the [§]Inflammation Program, The University of Iowa, Iowa City, Iowa 52242

Background: Endotoxin priming of neutrophils requires NADPH oxidase-derived reactive oxygen species, but localization of oxidant generation is unknown.
Results: NADPH oxidase is assembled and active on an endosomal compartment, and endocytosis is required for priming.
Conclusion: Intracellular oxidant signaling provides critical regulatory switch for neutrophil inflammatory state.
Significance: Modification of neutrophil activation may be advantageous to control host inflammation.

NADPH oxidase 2 (Nox2)-generated reactive oxygen species (ROS) are critical for neutrophil (polymorphonuclear leukocyte (PMN)) microbicidal function. Nox2 also plays a role in intracellular signaling, but the site of oxidase assembly is unknown. It has been proposed to occur on secondary granules. We previously demonstrated that intracellular NADPH oxidase-derived ROS production is required for endotoxin priming. We hypothesized that endotoxin drives Nox2 assembly on endosomes. Endotoxin induced ROS generation within an endosomal compartment as quantified by flow cytometry (dihydrorhodamine 123 and Oxyburst Green). Inhibition of endocytosis by the dynamin-II inhibitor Dynasore blocked endocytosis of dextran, intracellular generation of ROS, and priming of PMN by endotoxin. Confocal microscopy demonstrated a ROS-containing endosomal compartment that co-labeled with gp91^{phox}, p40^{phox}, p67^{phox}, and Rab5, but not with the secondary granule marker CD66b. To further characterize this compartment, PMNs were fractionated by nitrogen cavitation and differential centrifugation, followed by free flow electrophoresis. Specific subfractions made superoxide in the presence of NADPH by cell-free assay (cytochrome *c*). Subfraction content of membrane and cytosolic subunits of Nox2 correlated with ROS production. Following priming, there was a shift in the light membrane subfractions where ROS production was highest. CD66b was not mobilized from the secondary granule compartment. These data demonstrate a novel, nonphagosomal intracellular site for Nox2 assembly. This compartment is endocytic in origin and is required for PMN priming by endotoxin.

Priming of polymorphonuclear leukocytes (PMN)[2] in response to either host or foreign stimuli elicits an intermediate state of activation that alters subsequent responsiveness in terms of timing and intensity. The phenomenon of PMN priming is not purely an *in vitro* event but occurs *in vivo* in a number of clinical settings including during sepsis (1) and acute respiratory distress syndrome (2) and following traumatic injury (3). Although initial descriptions of neutrophil priming defined it as a preactivation state lacking NADPH oxidase 2 (Nox2) activity (4, 5), we (6, 7) and others (8–10) have demonstrated that low levels of reactive oxygen species (ROS) are generated in response to priming stimuli. Moreover, our data demonstrate that priming responses initiated by endotoxin and TNF-α are oxygen-dependent processes. Furthermore, these "priming" ROS are Nox2-derived and are required to elicit downstream primed responses. The precise location where these signaling ROS are generated has not been clearly defined.

The long-standing paradigm of Nox2 assembly and activation suggested that intracellular ROS were only generated in response to endocytosis of a particulate stimulus into the phagosome. However, there is growing acceptance that the phagocyte oxidase also generates low level ROS into a nonphagosomal compartment in response to certain stimuli and conditions (reviewed in Ref. 11). The nature of this compartment is still under investigation but has been suggested to be the secondary or specific granule (12), a reservoir for the majority of flavocytochrome b_{558} (cyt b_{558}) stores in unstimulated PMN. Possible alternatives that are discussed are the secretory vesicle compartment or a subset of these endocytic structures.

Although phagocytosis has been studied extensively, other forms of endocytosis have not been well characterized in PMN. Both fluid phase pinocytosis and clathrin-mediated uptake occur (13, 14), and the initiation of clathrin-mediated endocytosis by neutrophil priming agents has been characterized previously in response to platelet-activating factor (15). Furthermore, during priming of PMN by platelet-activating factor,

* This work was supported, in whole or in part, by National Institutes of Health Grants RO1AI073872 (to J. G. M.), AI079445 (to A. P. D. V.), RO1 HL62483 (to F. S. L.), and 2P01A104462011 (to J. G. M.).
[1] To whom correspondence may be addressed: Division of Critical Care, Dept. of Pediatrics, The University of Iowa, 200 Hawkins Dr., Iowa City, IA 52242. Tel.: 319-467-5042; Fax: 319-356-8443; E-mail: jessica-moreland@uiowa.edu.
[2] The abbreviations used are: PMN, polymorphonuclear leukocyte; Nox2, NADPH oxidase 2; ROS, reactive oxygen species; FFE, free flow electrophoresis, cyt b_{558}, flavocytochrome b_{558}; Oxyburst, OxyBURST Green® H_2HFF BSA; TR, Texas Red; LOS, lipooligosaccharide; TLR4-MD2, Toll-like receptor 4-lymphocyte antigen 96; LUC-CL, lucigenin-enhanced chemiluminescence; fMLF, formyl-Met-Leu-Phe; sCD14, soluble CD14; GTPγS, guanosine 5′-3-*O*-(thio)triphosphate.

assembly of a group of signaling proteins on the endosome is necessary for the primed phenotype to be generated (16). Endocytosis elicited during neutrophil priming by endotoxin has not been studied; however, in monocytes, lipopolysaccharide elicits formation of tubular invaginations and uptake of endotoxin occurs by both clathrin and non-clathrin-mediated pathways (17). Our previous data demonstrating a requirement for Nox2-derived ROS in priming suggested that the signaling ROS were generated intracellularly (6), and in the current study we sought to define the compartment where this occurs. Here, we demonstrate that endotoxin priming stimulates Nox2 assembly and activation on an endocytic vesicular structure in a subset of stimulated cells. This compartment is not distinct from the compartment that has been referred to as the secretory vesicles compartment but likely represents a subset of secretory vesicles. Moreover, endocytosis is required for generation of the primed phenotype. The process of priming alters the properties of the endocytic compartment in neutrophils as determined by free flow electrophoresis (FFE) separation of the light membranes. Although a small fraction of the secondary granule compartment is mobilized to the cell surface by endotoxin priming, this granule is not the site of intracellular ROS generation.

EXPERIMENTAL PROCEDURES

Materials—Hanks' balanced salt solution was obtained from Mediatech (Manassas, VA), human serum albumin was from Talecris Biotherapeutics (Durham, NC), paraformaldehyde was from Electron Microscopy Sciences (Hatfield, PA), Percoll and normal goat serum were from MP Biomedicals (Solon, OH), Ficoll-Paque was from GE Healthcare (Piscataway, NJ), dextran was from Pharmacosmos (Holbaek, Denmark), sucrose was from Fisher, and arachidonic acid was from Nu Chek Prep (Elysian, MN). Antibodies included anti-CD11b from Pharmingen (San Diego, CA), anti-CD66b from Abcam (Cambridge, MA) or Serotec (Raleigh, NC), anti-lactoferrin from Sigma, anti-p40^{phox} from Epitomics (Burlingame, CA), anti-p67^{phox} from BD Biosciences (San Jose, CA), anti-clathrin heavy chain from Santa Cruz Biotechnology (Santa Cruz, CA), and anti-gp91^{phox} (clone 7D5) from MBL International (Woburn, MA). Antibodies to p47^{phox} and the gp91^{phox} component of the cyt b_{558} (clone 54.1) were gifts from Dr. William Nauseef. Secondary antibodies were from Bio-Rad for immunoblotting, Invitrogen for confocal, and Jackson ImmunoResearch Laboratories (West Grove, PA) for flow cytometry. OxyBURST® Green H_2HFF BSA (Oxyburst), Alexa Fluor® 647 dextran, and Texas Red (TR) dextran were from Invitrogen. Lipooligosaccharide (LOS) purified from *Neisseria meningitides* was a gift from Dr. Jerrold Weiss. Additional reagents were obtained from Sigma. All of the buffers and reagents were strictly endotoxin-free.

Priming—As the stimulus for priming, a highly purified meningococcal endotoxin, LOS, in monomeric complex with soluble CD14 (cluster of differentiation 14), LOS-sCD14, was generated by the laboratory of Dr. Jerrold Weiss and used in our studies (18, 19). This complex allows specific cell activation via Toll-like receptor 4-lymphocyte antigen 96 (TLR4-MD2) to study the effect of endotoxin on cell activation.

Human PMN Purification—Human PMN were isolated according to standard techniques from heparin anti-coagulated venous blood from healthy consenting adults in accordance with a protocol approved by the Institutional Review Board for Human Subjects at the University of Iowa. PMN were isolated using dextran sedimentation and Ficoll-Paque density-gradient separation, followed by hypotonic lysis of erythrocytes as previously described (20).

Measurement of Intracellular ROS by Flow Cytometry—Freshly isolated PMN stimulated with LOS-sCD14 (10 ng/ml) or no agonist were incubated for 0–60 min in suspension at 37 °C in the presence of dihydrorhodamine 123 (130 μM). Immediately following the specified time points, the cells were placed on ice and analyzed by flow cytometry. In some experiments, the non-membrane-permeable Oxyburst (100 μg/ml) was used instead of dihydrorhodamine 123 to detect ROS present in endocytic compartments.

Measurement of Endocytosis of Texas Red Dextran by Flow Cytometry—PMN stimulated with LOS-sCD14 (10 ng/ml) or no agonist were incubated for 0–60 min in suspension at 37 °C in the presence of TR dextran (molecular weight, 10,000) (25 μg/ml). Immediately following the specified time points, the cells were placed on ice and washed to remove extracellular dextran prior to analysis by flow cytometry. In some experiments, the cells were pretreated with the dynamin-II inhibitor Dynasore (100–300 μM). In separate experiments, the cells were pretreated with chlorpromazine (40 μM for 30 min at room temperature) or sucrose (225 mM for 10 min at room temperature) as inhibitors of clathrin-mediated endocytosis (14). There was no alteration in PMN viability after treatment with these inhibitors.

Confocal Microscopy—PMN were incubated with LOS-sCD14 (10 ng/ml) or no agonist for 30 min in the presence of Oxyburst ± fluorescently labeled dextran either in suspension or after adhering to autologous serum-coated glass coverslips. The cells were then fixed in either ice-cold 4% paraformaldehyde for cells in suspension or in 10% formalin for adherent cells. The cells were viewed on a Zeiss LSM 510 Meta confocal microscope using a Plan-Apochromat 63×/1.4 oil DIC objective at room temperature with Zeiss Immersol 518 F halogen free/fluorescence free imaging medium. Oxyburst, Alexa Fluor 647, and TR fluorochromes were used for confocal microscopy. Pictures were taken with an AxioCam HR digital camera, and images were acquired with LSM 510 acquisition software. The images were processed with ImageJ.

Measurement of Nox2 Activity by Chemiluminescence—Lucigenin-enhanced chemiluminescence (LUC-CL) assays of Nox2 activity were performed in a 96-well plate using the FLUOstar Omega (BMG Labtech). 200 μl of a PMN suspension containing 2.5×10^6 PMN/ml in Hanks' balanced salt solution with 1% human serum albumin and 0.1% dextrose was added to each well with a final lucigenin concentration of 100 μM. The cells were stimulated by addition of LOS-sCD14 (10 ng/ml) ± formyl-Met-Leu-Phe (fMLF), as specified. Chemiluminescence was quantitated as relative luminescence units using a kinetic assay. For some experiments, the cells were pretreated with Dynasore (300 μM), chlorpromazine (40 μM), or sucrose (225 mM).

Analysis of Mobilization of Intracellular Protein Stores by Flow Cytometry—PMN at a concentration of 1×10^6/ml were analyzed using a FACScan flow cytometer (Becton-Dickinson). PMN were incubated in buffer or LOS-sCD14 as specified. Following incubation, PMN were resuspended in blocking buffer containing phosphate-buffered saline with 2% nonfat dry milk and 4% normal goat serum for 20 min on ice. Primary antibodies were added, including mouse IgG_1 control, anti CD11b, anti-gp91^{phox}, or anti-CD66b, all at final concentrations of 10 μg/ml, and incubated for 1 h on ice. The cells were centrifuged and resuspended in FITC-conjugated goat anti-mouse secondary antibody diluted 1:1000.

Subcellular Fractionation of Human PMN—Freshly isolated PMN were treated with the serine protease inhibitor diisopropyl fluorophosphate (1 mM) for 20 min at room temperature and centrifuged at 200 × *g* for 5 min at 4 °C. The cells were then incubated with LOS-sCD14 (10 ng/ml) or no agonist for 30 min in a 37 °C/5% CO_2 incubator followed by centrifugation at 200 × *g* for 5 min at 4 °C. The cells were resuspended in relaxation buffer (10 mM PIPES, 100 mM KCl, 3 mM NaCl, 3.5 mM $MgCl_2$, 1.25 mM ethyleneglycoltetraacetic acid) with 1 mM PMSF. The cells were placed in an ice-cold cell disruption vessel (Parr Instruments, Moline, IL) and closed tightly. The vessel was pressurized to 350 p.s.i. with nitrogen gas and allowed to equilibrate for 20 min at 4 °C. Cavitates were expelled dropwise into a tube containing ethyleneglycoltetraacetic acid (1.25 mM) and then centrifuged 200 × *g* for 10 min to remove unbroken cells and nuclei. Postnuclear supernatants were placed on top of two-layer Percoll gradients made as described (21) and centrifuged at 48,400 × *g* for 15 min at 4 °C in a Beckman Avanti J-25 centrifuge with low deceleration. Subcellular fractions were carefully removed from the gradient, and Percoll was removed by centrifugation. Sample buffer (62.5 mM Tris-HCl, pH 6.8, 5% β-mercaptoethanol, 2.3% SDS, 5% glycerol) was added to samples, which were then heated at 103 °C for 3 min prior to SDS-polyacrylamide gel electrophoresis.

High Voltage Free Flow Electrophoresis—FFE was used to separate the light membrane fractions into component parts using the γ-fraction isolated by two-layer Percoll density centrifugation as starting material (22). To reduce the surface charge on vesicles, the γ-fraction was treated with neuraminidase for 30 min at 37 °C at a final concentration of 0.2 units/ml by mixing 15 times with a 21-gauge needle. Following neuraminidase treatment, the samples were centrifuged at 184,000 × *g* for 15 min at 4 °C and resuspended in 750 μl of cold media buffer (6 mM triethanolamine and 6 mM glacial acetic acid, pH 7.4, with 270 mM sucrose and conductivity adjusted to 420 μS/cm). The electrode buffer consisted of 50 mM triethanolamine and 50 mM glacial acetic acid, pH 7.4. FFE was performed on a Becton-Dickinson free flow electrophoresis system (Sparks, MD) at 5 °C using a media flow rate of 300 ml/h and a sample flow rate of 3.5 ml/h. High voltage settings were 160 W, 1600 V, and 100 milliAmp to give constant amperage. Following separation by FFE, alkaline phosphatase activity assay was used to identify the orientation of light membrane vesicles within the 96 FFE fractions and thus to distinguish between plasma membrane vesicles and secretory vesicles (22). Briefly, 100 μl of each fraction collected by FFE was plated into duplicate 96-well microplates. 25 μl of 2% Triton X-100 was added to each well of one plate and incubated for 15 min at room temperature. 150 μl of 2.5 mg/ml *p*-nitrophenyl phosphate was added to each well and incubated for 30 min in the dark followed by reading on FLUOstar Omega at 405 nm. The 96 fractions collected by FFE were pooled into 12 groups consisting of 8 fractions each and concentrated to be used for further biochemical and functional analysis. Sample buffer was added to a portion of each fraction and heated prior to SDS-polyacrylamide gel electrophoresis, as above.

Protein Electrophoresis and Immunoblotting—Samples were resolved in an 8% gel by SDS-PAGE and then transferred to nitrocellulose. Immunoblots were processed using antibodies specific for the protein(s) of interest and species specific horseradish peroxidase-labeled secondary antibodies followed by enhanced chemiluminescence detection (Super Signal Substrate; Pierce). Immunoblots were scanned using the ImageQuant LAS-4000 imager (GE Healthcare), and relative abundances were quantitated using ImageQuant software.

Cell-free Assay of Nox2 Activity—1.5×10^7 cell equivalents of each FFE fraction were combined with fresh cytosol in a microplate well containing relaxation buffer, 100 μM cytochrome *c*, 55 μg/ml ATP, 50 μM GTPγS, and 100 μM arachidonic acid and mixed five times with a multichannel pipette. After a 4-min incubation at 37 °C, NADPH was added to a final concentration of 130 μg/ml, and the production of O_2^- was measured continuously at 550 nM for 20 min as the reduction of ferricytochrome *c* using the FLUOstar Omega (BMG Labtech).

RESULTS

Endotoxin Priming Elicits Intracellular ROS Production—Our initial manuscript demonstrating a requirement for Nox2-derived ROS for endotoxin priming included indirect evidence that these critical ROS were intracellular in location. We sought direct evidence for this contention using flow cytometry-based detection of the ROS-sensitive probe dihydrorhodamine 123. PMN in suspension displayed time-dependent acquisition of intracellular fluorescence that was significantly enhanced by incubation with priming concentrations of endotoxin (Fig. 1*A*). Although these data provide convincing evidence that intracellular ROS are elicited, the probe utilized is freely permeable and thus gives no evidence about the nature of the compartment. We hypothesized that the endosome was a likely location for nonphagosomal intracellular ROS generation and therefore repeated these flow cytometry-based experiments using the Oxyburst reagent conjugated to BSA. This probe cannot diffuse across membranes and thus must be actively taken up by endocytosis. In unstimulated PMN we saw minimal Oxyburst signal. However, we demonstrated time-dependent enhanced fluorescence in a subset of PMN with a significantly greater percentage of endotoxin-primed PMN acquiring Oxyburst positivity (Fig. 1, *B* and *C*). At 60 min, 81 ± 18.8% of endotoxin primed PMN had an Oxyburst-positive compartment.

Visualization of Intracellular ROS by Confocal Microscopy—To confirm our flow cytometry findings, we analyzed PMN for Oxyburst fluorescence by confocal microscopy. PMN were stimulated with LOS-sCD14 for 30 min in the presence of Oxyburst and also TR dextran to label the endocytic compartment.

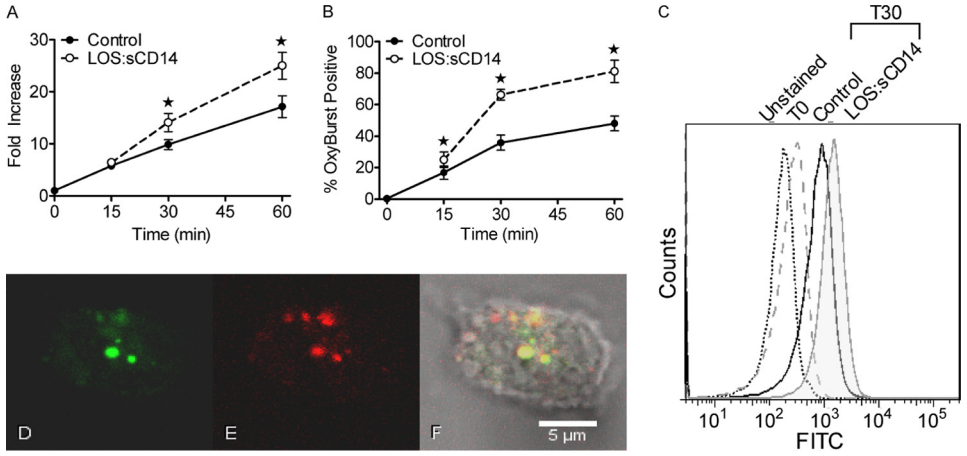

FIGURE 1. **Endotoxin priming elicits intracellular ROS production.** *A*, intracellular ROS were measured by flow cytometry using the cell permeable DHR 123 fluorescent ROS-sensitive probe. LOS:sCD14 10 ng/ml, elicited a time-dependent increase in intracellular ROS as compared to control. Control cells at time 0, immediately following addition of the probe, are set to a value of 1, and data are presented as fold-increase with respect to this value, * = $p < 0.05$, $n = 10$. *B*, using Oxyburst to measure intracellular ROS in endocytic compartments, LOS:sCD14-primed PMNs displayed a significantly greater percentage of Oxyburst positive cells than did control PMN, * = $p < 0.05$, $n = 6$. *C*, representative histogram from compiled data in *B*. *D–F*, confocal microscopy demonstrated Oxyburst positive vesicular compartments in a subset of cells. Representative confocal image of PMN after 30 min of priming with LOS:sCD14 demonstrating Oxyburst positive, ROS-containing vesicles (*D*), colocalizing with TR-dextran containing vesicles (*E*), and merged image (*F*).

By confocal microscopy, the majority of cells had endosomes filled with TR-dextran after 30 min. A subset of cells also demonstrated co-localization of Oxyburst and TR-dextran in a vesicular compartment (Fig. 1, *D–F*). The number of cells containing Oxyburst-positive vesicles increased over time and was similar to the quantitative flow cytometry data. These Oxyburst-positive PMN endosomes were easily distinguishable from the autofluorescent granules seen in eosinophils.

Evaluation of and Requirement for Endocytic Pathway in Endotoxin Priming—In view of the confocal microscopy findings, we next sought to quantitatively evaluate endocytosis in endotoxin-primed PMN. Using flow cytometry analysis of TR-dextran, time-dependent acquisition of intracellular dextran was noted in unstimulated cells, and dextran acquisition was significantly enhanced by priming with endotoxin at all time points from 15 to 60 min (Fig. 2*A*). To investigate the requirement for endocytosis in the priming process, we tested the dynamin-II inhibitor Dynasore for its ability to block TR-dextran endocytosis under both constitutive and endotoxin-primed conditions. In preliminary studies, we tested a range of concentrations of the inhibitor based on the wide range utilized in the literature (23, 24). We found that 100 μM Dynasore was sufficient to block the constitutive endocytosis seen in unstimulated PMN, and higher concentrations were required to block the endotoxin-mediated enhancement of dextran endocytosis (data not shown). At the 30- and 60-min time points, Dynasore (300 μM) significantly inhibited endocytosis of dextran in unstimulated PMN as well as endotoxin-stimulated conditions (Fig. 2*B*). Using this concentration of Dynasore, we studied priming of the respiratory burst in response to fMLF. Because this dynamin-II inhibitor is fully reversible, we treated cells with Dynasore during the priming period and then washed cells to remove the inhibitor prior to analysis of primed Nox2 activity. Under these conditions, Dynasore-pretreated cells displayed markedly reduced priming of the fMLF-elicited respiratory burst with an average 1.9-fold reduction in the peak Nox2 activity to fMLF (Fig. 2*C*) but had normal responsiveness

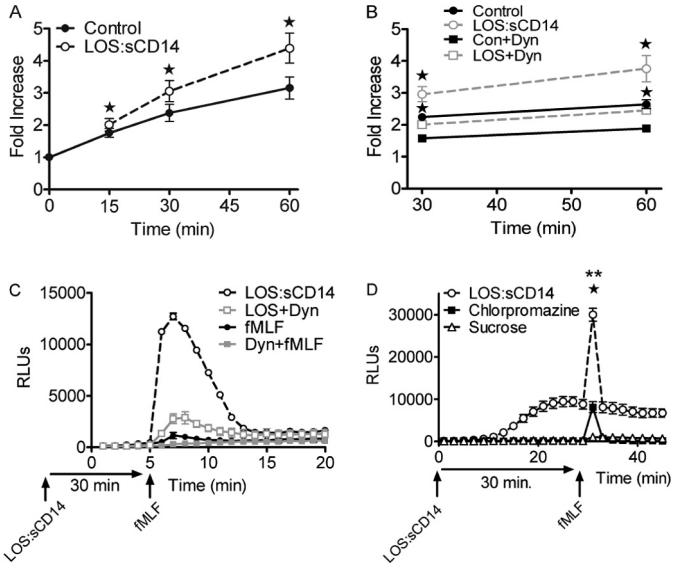

FIGURE 2. **Endotoxin priming elicits endocytosis, and endocytosis is required for priming of the respiratory burst.** *A*, flow cytometry analysis of endocytosis of TR-dextran in control *versus* LOS:sCD14-treated PMN demonstrates a significant increase in endocytosis in response to priming. Fold increase presented with respect to control cells at time 0, * = $p < 0.05$, $n = 5$. *B*, effect of the dynamin-II inhibitor Dynasore on endocytosis of TR dextran in control *versus* LOS:sCD14 PMNs. Dynasore (Dyn, 300 μM) significantly inhibits constitutive endocytosis in unstimulated PMNs. Dynasore also blocked LOS:sCD14-mediated enhancement of TR-dextran endocytosis, * = $p < 0.05$, $n = 6$. *C*, PMN were primed with LOS:sCD14 in the absence or presence of Dynasore for 30 min before washing twice and then stimulating with fMLF. Primed NADPH oxidase activity, as measured by LUC-CL, in response to fMLF was markedly inhibited in the cells primed in the presence of Dynasore, representative tracing, $n = 8$. *D*, both chlorpromazine (40 μM) and sucrose (225 mM) significantly inhibited LOS:sCD14-primed NADPH oxidase activity, as measured by LUC-CL, in response to fMLF. ** = $p < 0.05$ sucrose compared to LOS:sCD14 without inhibitor, * = $p < 0.05$ for chlorpromazine compared to no inhibitor, $n = 8$.

to PMA. We next investigated the effect of two inhibitors of clathrin-mediated endocytosis, chlorpromazine, and sucrose. Preincubation with either agent significantly inhibited endotoxin-mediated endocytosis but had no significant effect on constitutive endocytosis (data not shown, $n = 8$). There was no

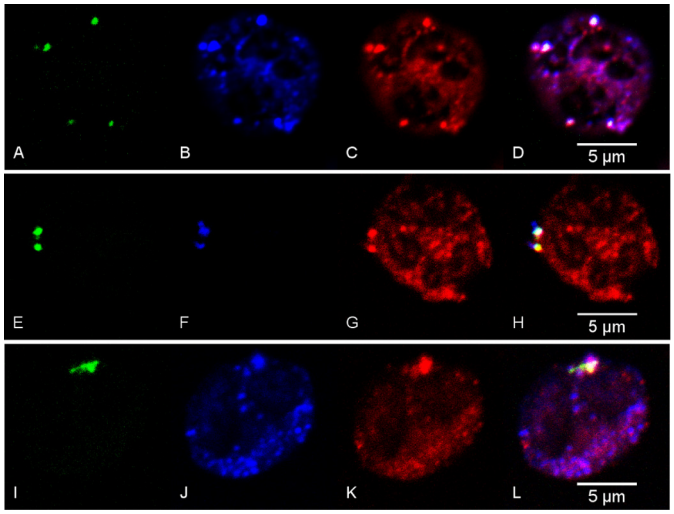

FIGURE 3. **Confocal microscopy analysis of endotoxin primed PMN displays ROS-containing vesicles that colocalize with NADPH oxidase components and early endosomal markers.** PMNs were incubated for 30 min with LOS:sCD14 (10 ng/ml) in the presence of the ROS-sensitive probe, Oxyburst, and Alexa Fluor 647 dextran. Oxyburst positive, ROS-containing vesicles are seen in *green* (*A*, *E*, *I*) and colocalize with gp91^{phox} in *blue* (*B*, *J*), Alexa Fluor 647 dextran in *blue* (*F*), p40^{phox} (*C*), p67^{phox} (*G*), and rab5 (*K*), all in *red*. *D*, *H*, *L*, representative merged images.

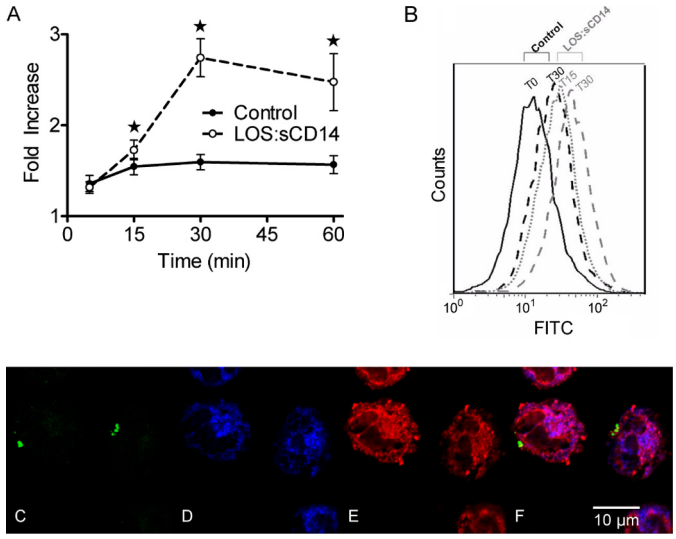

FIGURE 4. **Endotoxin priming elicits low-level mobilization of secondary granules to the cell surface, but ROS-containing endosomes do not express secondary granule markers.** *A*, cell surface levels of CD66b are significantly enhanced by priming with LOS:sCD14, 10 ng/ml, as compared to control conditions, * = $p < 0.05$, $n = 9$. *B*, representative flow cytometry histogram of CD66b. *C–F*, confocal microscopy of endotoxin primed PMNs display Oxyburst positive, ROS-containing vesicles (*C*). Robust staining for the secondary granule markers (*D*) CD66b (*blue*), and (*E*) lactoferrin (*red*) is present in all cells, but there is no colocalization of ROS-positive vesicles with either CD66b or lactoferrin (*F*). Representative merged image is from 4 independent experiments.

effect on PMN viability at the concentrations utilized. Pretreatment of PMNs with either chlorpromazine or sucrose profoundly inhibited endotoxin priming of the fMLF-elicited respiratory burst (Fig. 2*D*). Considered in combination, these data provide evidence that endotoxin priming enhances dynamin-II-dependent and clathrin-mediated endocytosis and that endocytosis is necessary for PMN to develop the primed phenotype.

Further Characterization of Endosomal ROS-containing Compartment—Next we focused on demonstrating the presence of Nox2 components on these endosomal ROS containing vesicles. Using confocal microscopy we noted that gp91^{phox} co-localized on many vesicles that were Oxyburst-positive, in addition to being seen in a wide distribution throughout the cell. Many ROS containing vesicles also displayed p40^{phox}, which was expected in view of recent data demonstrating a specific role for p40^{phox} in intracellular ROS generation (Fig. 3, *A–D*) (25). p67^{phox} was also present on the ROS-positive, dextran-containing endocytic vesicles under investigation (Fig. 3, *E–H*). Although markers of the endocytic pathway have not been fully characterized in PMN, we looked for co-localization of Rab5, a well described early endosomal protein, with the Nox2-positive, ROS-containing vesicles. Rab5 was noted to be overlapping strongly with dextran-containing endocytic vesicles (data not shown) and co-localized with gp91^{phox} and Oxyburst in the subset of vesicles that were ROS-positive (Fig. 3, *I–L*).

Because it has been suggested previously that the secondary granule is the site of intracellular Nox2 assembly and ROS generation (8, 12, 26), we explored the effect of endotoxin priming on specific or secondary granule exocytosis using CD66b as a membrane marker for secondary granules. Using flow cytometry of live cells, we initially sought to determine whether there is mobilization/exocytosis of this granule population in response to the priming stimulus alone. In response to endotoxin, PMN demonstrated a significant increase in CD66b levels on the cell surface at 30 min (Fig. 4, *A* and *B*), suggesting that this granule population is partially mobilized in response to endotoxin alone. Next, using confocal microscopy, we utilized two markers of secondary granules: CD66b as the membrane marker and lactoferrin as a soluble protein. We investigated whether CD66b and lactoferrin are present on the endosomal ROS-containing compartment under investigation. Although there was robust and overlapping staining for CD66b and lactoferrin in unstimulated PMNs (data not shown), there was no evidence of any co-localization of either CD66b or lactoferrin with the ROS-containing endosomes where Nox2 was assembled (Fig. 4, *C–F*). Taken together, these data suggest that endotoxin priming stimulates assembly and activation of the Nox2 on a vesicular compartment with characteristics of an early endosome rather than on a secondary granule.

Biochemical Analysis of Endosomal Vesicle Population—We have previously used nitrogen cavitation, followed by Percoll density gradient centrifugation to isolate purified subcellular fractions from unstimulated PMN to characterize the localization of proteins within the PMN (28). We hypothesized that if either the endosomal compartment or the secondary granule was the location of Nox2 assembly, then we could reliably separate these subfractions and study mobilization of the cytosolic subunits of the oxidase to this subfraction. Consistent with previously published reports (21) we found that 72.1 ± 3.1% ($n = 6$) of the total cellular gp91^{phox} was in the secondary granule fraction in resting cells, with the remainder in the light membrane fraction, which includes both plasma membrane vesicles and secretory vesicles (or endosomes). The compartmental localization of gp91^{phox} was not significantly altered following endo-

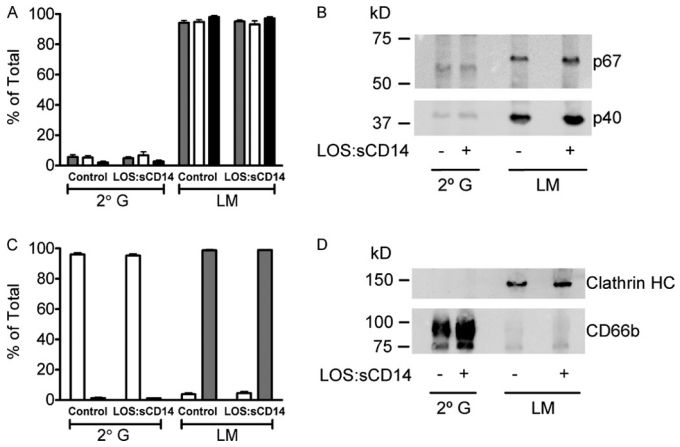

FIGURE 5. **NADPH oxidase cytosolic subunits are associated with the light membrane (LM) fraction, but not the secondary granule (2° G) fraction, isolated from both control and endotoxin-primed PMN.** *A–B*, control and LOS:sCD14-primed (10 ng/ml) PMN were subjected to cavitation and Percoll density gradient centrifugation with isolation of each of the granule fractions. LM and 2° G subfractions were immunoblotted for p40^{phox} (*grey-filled bars*), p47^{phox} (*open bars*), and p67^{phox} (*black bars*). Greater than 90% of the Nox2 cytosolic subunit proteins, which were membrane-associated, were found associated with the LM fraction. There was no increase in cytosolic subunit abundance associated with the LM subfraction following endotoxin priming. Data were compiled from $n = 5–6$ individual experiments. *B*, representative immunoblot displaying p67^{phox} and p40^{phox}. *C*, immunoblotting for the 2° G marker CD66b (*open bars*) displayed minimal mobilization from the 2° G fraction to the LM fraction after priming with LOS:sCD14. Immunoblotting for clathrin heavy chain (*grey-filled bars*) demonstrated significant association of clathrin with the LM fraction but none associated with the 2° G compartment, $n = 4$. *D*, representative immunoblot displaying clathrin HC and CD66b.

toxin priming with 77.9 ± 3.5% in the secondary granule fraction and 22.1 ± 3.5% in the light membrane fraction. Because gp91^{phox} is one of the membrane components of the oxidase, these results were expected. We next studied the control *versus* endotoxin-primed subcellular fractions for biochemical evidence of localization of the cytosolic subunits, p67^{phox}, p47^{phox}, and p40^{phox}, as had been seen by confocal microscopy. Approximately 95% of the membrane-associated p47^{phox} was found associated with the light membranes, whereas minimal p47^{phox} was detected in association with the secondary granule fraction. A similar pattern was seen for p40^{phox} and p67^{phox}. Following 30 min of endotoxin priming, there was no significant change in the relative proportion of cytosolic subunit proteins associated with the secondary granule *versus* light membrane subfractions. These data provide additional evidence that the secondary granules are not the site of Nox2 assembly under endotoxin-priming conditions (Fig. 5, *A* and *B*). The vast majority of total cellular stores of the Nox2 cytosolic subunits remained in the cytosol, thus making it very difficult to discern whether endotoxin priming had mobilized a greater amount from the cytosolic compartment to the light membranes, as compared with localization in nonprimed cells. We went on to study the CD66b content of these fractions and found that >95% of total cellular CD66b was retained in the secondary granule fraction following endotoxin priming, indicating that the increased surface expression demonstrated by flow cytometry (Fig. 4, *A* and *B*) represented a very small proportion of the total cellular CD66b (Fig. 5, *C* and *D*). Additionally, we analyzed these fractions for clathrin content, because the light membrane fraction was expected to contain endosomes generated by clathrin-mediated endocytosis. The light membrane fraction of both control and endotoxin-primed PMN had clathrin protein detectable by immunoblotting, whereas clathrin was virtually undetectable in the secondary granule fraction (Fig. 5, *C* and *D*).

Although these immunoblotting analyses demonstrated the presence of many expected proteins in the light membrane subfraction, there were no detectable differences between control and endotoxin-primed vesicles. We elected to purify the light membrane fraction further using high voltage FFE, which separates the light membranes into 96 subfractions based on size and charge. This approach has been extensively described and characterized as a method to separate PMN plasma membrane vesicles from secretory vesicles by performing an alkaline phosphatase assay on the isolated FFE fractions (21, 22). Under control conditions, plasma membrane vesicles (generated outside-out by cavitation) are identified by alkaline phosphatase enzyme positivity on the extravesicular surface, *i.e.* without any further permeabilization. In contrast, secretory vesicles (outside-in endosomes) have "latent" alkaline phosphatase activity that is observed only following permeabilization with Triton X-100. In view of our data demonstrating marked enhancement of PMN endocytosis in response to endotoxin, we postulated that priming would alter the characteristics of these subcellular vesicular populations. We isolated 96 fractions as described from control *versus* endotoxin-primed PMN and analyzed the expression of alkaline phosphatase on these vesicle subfractions. The distribution of alkaline phosphatase activity in the post FFE subfractions were clearly shifted in response to endotoxin priming (Fig. 6*A*). This indicates alterations in the size, charge, or surface properties of the primed endosomal population. This shift in fraction properties was highly reproducible across multiple experiments.

We elected to pool groups of these 96 fractions for further functional and biochemical analysis and generated 12 groups of eight fractions from each FFE sample. We again analyzed these subfractions for expression of membrane and cytosolic components of the Nox2 complex. In control PMN, gp91^{phox} was present predominantly in pooled subfractions 3–5 with a peak in fraction 4. However, following endotoxin priming, the gp91^{phox} was shifted toward fraction 5 (Fig. 6, *B* and *C*). Minimal protein was detected in subfractions 9–12, so immunoblots demonstrate only the first eight pooled fractions. Immunoblot analysis of the Nox2 cytosolic subunits within the pooled subfractions paralleled our findings with gp91^{phox} with a significant shift following endotoxin priming. This shift was more pronounced for p40^{phox} and p67^{phox} than for p47^{phox} (Fig. 6, *D–G*). Interestingly, there was no shift in the clathrin band across subfractions between control and endotoxin-primed PMN, suggesting that the shift was not due to a global alteration in the migration of subcellular vesicles during FFE following endotoxin priming, but rather a specific compositional change in the subset of endosomes containing the Nox2, *i.e.* redistribution of Nox2 within the compartment as a result of priming (Fig. 6, *H* and *I*).

Functional Analysis of Endosomal Vesicles after Priming—The isolated light membrane subfraction has been utilized by many laboratories (29–31) to study the function of the Nox2 using a cell-free assay of superoxide production. We postulated that the pooled subfractions generated following separation by

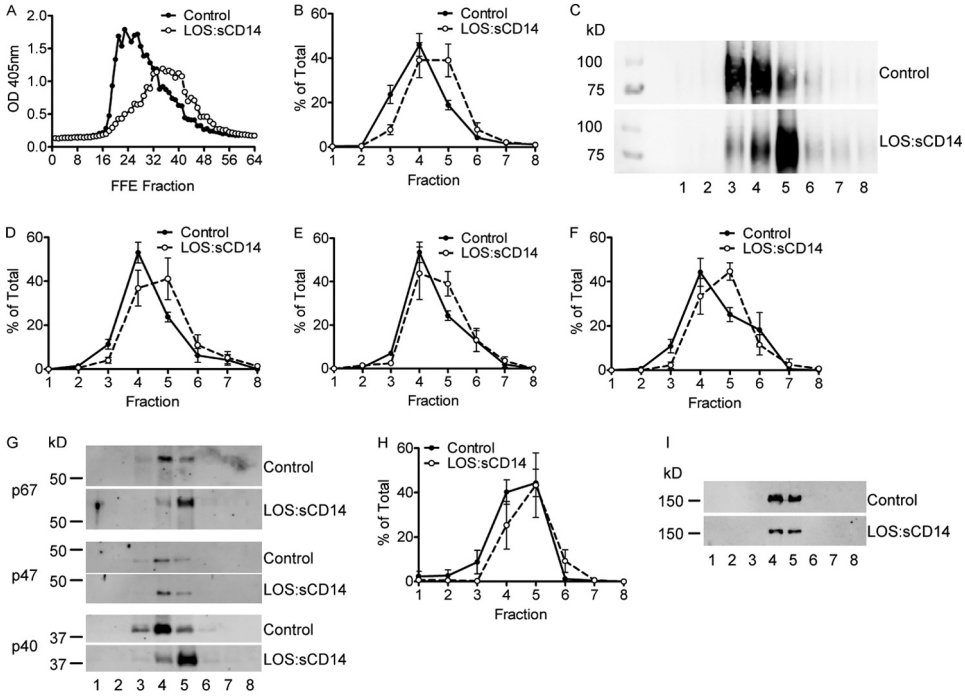

FIGURE 6. **Endotoxin priming of PMN elicits an alteration in the properties of the light membrane subfractions.** *A*, alkaline phosphatase activity assay performed on the FFE subfractions from control and endotoxin-primed, 10 ng/ml LOS:sCD14. PMN demonstrates a shift in the fractions displaying alkaline phosphatase activity post-Triton X-100 permeabilization, representative activity assay, from $n = 5$ individual experiments. FFE subfractions were pooled into groups of 8 for further biochemical analysis. *B–C*, gp91^{phox} protein was detected primarily in pooled subfractions 3, 4, and 5 from control PMNs, but shifted to fractions 4, 5, and 6 following endotoxin priming. *B*, compiled data from $n = 5$ separate FFE runs. *C*, representative immunoblot for gp91^{phox}. *D–F*, cytosolic subunits of the oxidase were also associated with light membrane pooled subfractions isolated by FFE. p40^{phox} (*D*) and p67^{phox} (*F*) displayed similar shifts by immunoblotting as seen with gp91^{phox}, whereas p47^{phox} (*E*) had only a minor shift following priming, $n = 5$. *G*, representative immunoblot for control *versus* LOS:sCD14 primed PMNs for cytosolic subunits of Nox2. *H–I*, there was no shift in the clathrin heavy chain protein content of FFE subfractions following endotoxin priming, $n = 5$.

FFE would retain this functional capacity. Furthermore, we hypothesized that the shift in Nox2 subunit proteins detected by immunoblotting after endotoxin priming would be mirrored in the superoxide-generating activity of each pool. Using equal amounts of membrane fraction from each of the first eight pooled subfractions, we analyzed the reduction of ferricytochrome *c* as a measure of Nox2 activity. Following FFE, the isolated vesicles were functionally active using the cell-free system. Compared with control PMN fractions, following endotoxin-priming, there was a clear shift in the fractions with the greatest levels of Nox2 activity as measured by superoxide generation (Fig. 7). These data provided functional confirmation that endotoxin priming alters the Nox2 activity of PMN endosomal vesicles.

DISCUSSION

Nox2-dependent generation of superoxide into the PMN phagosome following ingestion of microbes or other particulate stimuli has been extensively studied and characterized. Similarly, assembly and activation of the Nox2 complex at the neutrophil plasma membrane in response to a soluble agonist has been described in detail. However, despite solid evidence that other members of the Nox family generate ROS into intracellular vesicular compartments (32, 33), there has been only limited investigation of the possibility that the Nox2 assembles on an intracellular, nonphagosomal membrane for ROS generation. We became interested in Nox2-derived ROS signaling in PMN after demonstrating that endotoxin priming of neutrophils is an oxygen-dependent process and specifically requires Nox2-derived ROS (6).

In the current investigation, we provide evidence for two novel findings related to the function of the PMN Nox2. First, the Nox2 complex is assembled on endosomes in response to priming concentrations of endotoxin and is activated to generate intraendosomal ROS. Second, endocytosis is a required element of priming for PMN development of the primed phenotype. To our knowledge, this is the first description of assembly and activation of Nox2 on an endosome. Our data support the contention that this endosomal compartment is a subset of the compartments that have been broadly termed secretory vesicles within the PMN literature. Initial descriptions of nonphagosomal intracellular ROS generation in PMN were generally focused on cellular responses to the phorbol ester PMA and identified the secondary granule as the likely compartment of assembly (8, 12, 26). More recently, assembly of the PMN oxidase has been described on a vesicular "prephagosomal" compartment during Fc receptor-mediated phagocytosis (34). This compartment subsequently fused with the phagosome. The functional significance of this compartment is not entirely clear, but interesting questions about spatial delivery of redox signaling were raised. Herein, using several complementary assays, we demonstrate that intracellular, endosomal Nox2-dependent generation of ROS is initiated by cell stimulation with endotoxin, requires endocytosis, and does not involve the secondary granule membrane.

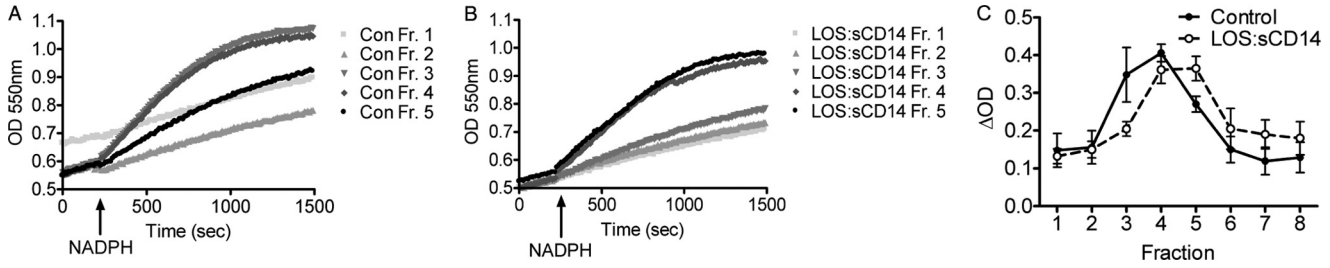

FIGURE 7. **Cell-free NAPDH oxidase assay for measurement of superoxide production using the reduction of ferricytochrome *c* displays a shift in the superoxide generating fractions following endotoxin priming.** *A*, in control PMN, pooled subfractions 3 and 4 generated the greatest amount of superoxide following addition of NADPH, whereas peak superoxide generating activity shifted to subfractions 4 and 5 following endotoxin priming (*B*). *C*, compiled data for superoxide generation by subfractions from $n = 3$ FFE experiments comparing control *versus* endotoxin-primed PMN displays a full fraction shift in peak superoxide generating activity.

From a mechanistic perspective, alterations in localization and phosphorylation status of subunits of the oxidase complex have been described to play a role in the development of the primed state. Phosphorylation of $p47^{phox}$ has been extensively studied in response to both priming and activating stimuli, and sequential phosphorylation events appear to occur (35) during the course of assembly and activation. Phosphorylation of Ser-345 on $p47^{phox}$ is a necessary event in priming of neutrophils by TNF-α and GM-CSF (36, 37). During endotoxin priming, partial phosphorylation of $p47^{phox}$ has been reported, although the specific residues have not been identified (38), and translocation of this subunit to the plasma membrane also occurs. Endotoxin priming elicits a quantitative increase in intracellular endosomal ROS. Although the properties of the light membrane compartment were clearly altered, we observed no quantitative difference in the percentage of the cytosolic subunits that localized there. These data suggest a qualitative alteration in the oxidase assembled in the primed cells. The relative phosphorylation state of each of the relevant subunits is currently under investigation in isolated light membranes of endotoxin-primed *versus* control PMN.

Moreover, our data provide solid evidence that endotoxin priming does not mobilize additional stores of cyt b_{558} from the secondary granule compartment to the light membrane compartment. Based on our method of differential centrifugation, our data would also exclude mobilization of additional cyt b_{558} from the gelatinase-positive tertiary granule compartment, as has been described for priming by G-CSF (39). Rather, endotoxin elicits a functional reorganization of the membrane Nox2 that is present initially in the light membranes (plasma membrane and secretory vesicles). From the early work of Borregaard and co-workers, later confirmed by others, it is apparent that 80–85% of the PMN cyt b_{558} exists in the secondary granule compartment, with the remainder in light membrane compartment of resting cells, divided between secretory vesicles and the plasma membrane (21, 22). We demonstrated a similar distribution between secondary granules and light membranes in our control PMN population. This distribution was not altered by endotoxin priming. We speculate that by eliciting endocytosis, endotoxin shifts cyt b_{558} out of the plasma membrane into vesicles having a distinct lipid composition. However, these endosomes remain within the light membrane fraction, thus preventing a change in the overall distribution of the cytochrome. In addition, endotoxin stimulation likely produces quantitative and qualitative changes in the signaling proteins that are incorporated into endosomes. These two factors may explain the altered distribution of the physical properties of the light membrane vesicle populations as assessed by electrophoresis.

In broad terms, it is not clear exactly which form(s) of endocytosis is/are necessary for the priming of neutrophils to proceed. We utilized a low molecular weight dextran that would be easily taken up during clathrin-mediated endocytosis, and this is the described mechanism for uptake of endotoxin bound to the TLR4-MD2 complex (40). Although not studied to date in neutrophils, uptake of endotoxin-TLR4-MD2 into an endocytic compartment has been described extensively in many cell types, including monocytes (41) and macrophages (42). Endocytosis of the complex was initially characterized as a mechanism for termination or deactivation of endotoxin signaling and targeting for ubiquitination (40). More recently, there has been evidence that TLR4 signaling via MyD88 occurs at the plasma membrane, whereas MyD88-independent (IRF3 pathway) signaling occurs in an endosomal location (43). There are few data on proximal endotoxin signaling in PMN, with a single study suggesting that the IRF3 pathway is not activated by endotoxin (44). Although we did not specifically explore the uptake of endotoxin in the current study, we speculate that the endocytic ROS-containing compartment identified will contain endotoxin bound to TLR4-MD2. We are actively investigating the uptake and processing of endotoxin in PMN, with a specific focus on the question of whether the mode of presentation of endotoxin impacts the compartment and signaling elicited.

The mechanisms and regulation of neutrophil priming by both bacterial and host products have been a focal area for our laboratory in recent years. Considered in combination with our recently published studies on TNF-α-mediated neutrophil signaling (7), the data presented here suggest a new role for Nox2 in intracellular signaling. The relevance of understanding the mechanisms of PMN priming in relationship to human disease processes has been progressively delineated. Many years ago, *in vivo* primed neutrophils were identified in patients with the acute respiratory distress syndrome (2), sepsis (1), and following traumatic injury (3), although these early reports failed to identify a causal link between priming and outcome. More recently, priming of neutrophils in the peripheral blood of patients with chronic inflammatory diseases, including rheumatoid arthritis, chronic kidney disease, and inflammatory bowel disease (45–47), has been identified. These findings suggest that therapeutic control of neutrophil priming might pro-

vide a new approach to the management of chronic inflammation.

In summary, the current manuscript describes and characterizes a novel compartment for Nox2 assembly that is necessary for PMN priming. We hypothesize that the endosomal localization of these Nox2-derived ROS provides a regulated delivery system whereby oxidant sensitive proteins can be modified in a spatially and temporally segregated manner without damaging effects on the rest of the cell. Our long-standing interest in the interaction between the anion-proton antiporter, ClC-3, and the NADPH oxidase (6, 27) may be explained by events specific to the endosome but not relevant at the phagosomal or plasma membrane. These endosomally specific ROS are required for PMN priming and represent a target area for therapeutic intervention, potentially via targeted inhibition of ClC-3.

Acknowledgments—We thank Dr. Jerrold Weiss and Dr. Theresa Gioannini for generously providing the endotoxin-sCD14 complex used for priming and Dr. William Nauseef for antibodies to subunits of Nox2.

REFERENCES

1. Bass, D. A., Olbrantz, P., Szejda, P., Seeds, M. C., and McCall, C. E. (1986) Subpopulations of neutrophils with increased oxidative product formation in blood of patients with infection. *J. Immunol.* **136,** 860–866
2. Chollet-Martin, S., Montravers, P., Gibert, C., Elbim, C., Desmonts, J. M., Fagon, J. Y., and Gougerot-Pocidalo, M. A. (1992) Subpopulation of hyperresponsive polymorphonuclear neutrophils in patients with adult respiratory distress syndrome. Role of cytokine production. *Am. Rev. Respir. Dis.* **146,** 990–996
3. Ogura, H., Tanaka, H., Koh, T., Hashiguchi, N., Kuwagata, Y., Hosotsubo, H., Shimazu, T., and Sugimoto, H. (1999) Priming, second-hit priming, and apoptosis in leukocytes from trauma patients. *J. Trauma* 46, 774–783
4. Condliffe, A. M., Kitchen, E., and Chilvers, E. R. (1998) Neutrophil priming. Pathophysiological consequences and underlying mechanisms. *Clin. Sci.* **94,** 461–471
5. Swain, S. D., Rohn, T. T., and Quinn, M. T. (2002) Neutrophil priming in host defense. Role of oxidants as priming agents. *Antioxid. Redox Signal.* **4,** 69–83
6. Moreland, J. G., Davis, A. P., Matsuda, J. J., Hook, J. S., Bailey, G., Nauseef, W. M., and Lamb, F. S. (2007) Endotoxin priming of neutrophils requires NADPH oxidase-generated oxidants and is regulated by the anion transporter ClC-3. *J. Biol. Chem.* **282,** 33958–33967
7. Volk, A. P., Barber, B. M., Goss, K. L., Ruff, J. G., Heise, C. K., Hook, J. S., and Moreland, J. G. (2011) Priming of neutrophils and differentiated PLB-985 cells by pathophysiological concentrations of TNF-α is partially oxygen dependent. *J. Innate Immun.* **3,** 298–314
8. Kobayashi, T., Robinson, J. M., and Seguchi, H. (1998) Identification of intracellular sites of superoxide production in stimulated neutrophils. *J. Cell Sci.* **111,** 81–91
9. Brown, G. E., Stewart, M. Q., Liu, H., Ha, V. L., and Yaffe, M. B. (2003) A novel assay system implicates PtdIns(3,4)P_2, PtdIns(3)P, and PKCδ in intracellular production of reactive oxygen species by the NADPH oxidase. *Mol. Cell* **11,** 35–47
10. Ambruso, D. R., Cusack, N., and Thurman, G. (2004) NADPH oxidase activity of neutrophil specific granules. Requirements for cytosolic components and evidence of assembly during cell activation. *Mol. Genet. Metab.* **81,** 313–321
11. Bylund, J., Brown, K. L., Movitz, C., Dahlgren, C., and Karlsson, A. (2010) Intracellular generation of superoxide by the phagocyte NADPH oxidase. How, where, and what for? *Free Radic. Biol. Med.* **49,** 1834–1845
12. Karlsson, A., and Dahlgren, C. (2002) Assembly and activation of the neutrophil NADPH oxidase in granule membranes. *Antioxid. Redox Signal.* **4,** 49–60
13. Eckels, P. C., Banerjee, A., Moore, E. E., McLaughlin, N. J., Gries, L. M., Kelher, M. R., England, K. M., Gamboni-Robertson, F., Khan, S. Y., and Silliman, C. C. (2009) Amantadine inhibits platelet-activating factor induced clathrin-mediated endocytosis in human neutrophils. *Am. J. Physiol. Cell Physiol.* **297,** C886–C897
14. Uriarte, S. M., Jog, N. R., Luerman, G. C., Bhimani, S., Ward, R. A., and McLeish, K. R. (2009) Counterregulation of clathrin-mediated endocytosis by the actin and microtubular cytoskeleton in human neutrophils. *Am. J. Physiol. Cell Physiol.* **296,** C857–C867
15. McLaughlin, N. J., Banerjee, A., Kelher, M. R., Gamboni-Robertson, F., Hamiel, C., Sheppard, F. R., Moore, E. E., and Silliman, C. C. (2006) Platelet-activating factor-induced clathrin-mediated endocytosis requires β-arrestin-1 recruitment and activation of the p38 MAPK signalosome at the plasma membrane for actin bundle formation. *J. Immunol.* **176,** 7039–7050
16. McLaughlin, N. J., Banerjee, A., Khan, S. Y., Lieber, J. L., Kelher, M. R., Gamboni-Robertson, F., Sheppard, F. R., Moore, E. E., Mierau, G. W., Elzi, D. J., and Silliman, C. C. (2008) Platelet-activating factor-mediated endosome formation causes membrane translocation of $p67^{phox}$ and $p40^{phox}$ that requires recruitment and activation of p38 MAPK, Rab5a, and phosphatidylinositol 3-kinase in human neutrophils. *J. Immunol.* **180,** 8192–8203
17. Kitchens, R. L., Wang, P., and Munford, R. S. (1998) Bacterial lipopolysaccharide can enter monocytes via two CD14-dependent pathways. *J. Immunol.* **161,** 5534–5545
18. Gioannini, T. L., Teghanemt, A., Zarember, K. A., and Weiss, J. P. (2003) Regulation of interactions of endotoxin with host cells. *J. Endotoxin Res.* **9,** 401–408
19. Gioannini, T. L., Zhang, D., Teghanemt, A., and Weiss, J. P. (2002) An essential role for albumin in the interaction of endotoxin with lipopolysaccharide-binding protein and sCD14 and resultant cell activation. *J. Biol. Chem.* **277,** 47818–47825
20. Boyum, A. (1968) Scandinavian journal of clinical and laboratory investigation. **97,** 77–89
21. Borregaard, N., Heiple, J. M., Simons, E. R., and Clark, R. A. (1983) Subcellular localization of the b-cytochrome component of the human neutrophil microbicidal oxidase. Translocation during activation. *J. Cell Biol.* **97,** 52–61
22. Sengeløv, H., Nielsen, M. H., and Borregaard, N. (1992) Separation of human neutrophil plasma membrane from intracellular vesicles containing alkaline phosphatase and NADPH oxidase activity by free flow electrophoresis. *J. Biol. Chem.* **267,** 14912–14917
23. Huang, Y. W., Su, P., Liu, G. Y., Crow, M. R., Chaukos, D., Yan, H., and Robinson, L. A. (2009) Constitutive endocytosis of the chemokine CX3CL1 prevents its degradation by cell surface metalloproteases. *J. Biol. Chem.* **284,** 29644–29653
24. Yamada, H., Abe, T., Li, S. A., Masuoka, Y., Isoda, M., Watanabe, M., Nasu, Y., Kumon, H., Asai, A., and Takei, K. (2009) Dynasore, a dynamin inhibitor, suppresses lamellipodia formation and cancer cell invasion by destabilizing actin filaments. *Biochem. Biophys. Res. Commun.* **390,** 1142–1148
25. Matute, J. D., Arias, A. A., Wright, N. A., Wrobel, I., Waterhouse, C. C., Li, X. J., Marchal, C. C., Stull, N. D., Lewis, D. B., Steele, M., Kellner, J. D., Yu, W., Meroueh, S. O., Nauseef, W. M., and Dinauer, M. C. (2009) A new genetic subgroup of chronic granulomatous disease with autosomal recessive mutations in $p40^{phox}$ and selective defects in neutrophil NADPH oxidase activity. *Blood* **114,** 3309–3315
26. Vaissiere, C., Le Cabec, V., and Maridonneau-Parini, I. (1999) NADPH oxidase is functionally assembled in specific granules during activation of human neutrophils. *J. Leukocyte Biol.* **65,** 629–634
27. Matsuda, J. J., Filali, M. S., Moreland, J. G., Miller, F. J., and Lamb, F. S. (2010) Activation of swelling-activated chloride current by tumor necrosis factor-alpha requires ClC-3-dependent endosomal reactive oxygen production. *J. Biol. Chem.* **285,** 22864–22873
28. Moreland, J. G., Davis, A. P., Bailey, G., Nauseef, W. M., and Lamb, F. S. (2006) Anion channels, including ClC-3, are required for normal neutrophil oxidative function, phagocytosis, and transendothelial migration.

J. Biol. Chem. **281,** 12277–12288
29. McPhail, L. C., Shirley, P. S., Clayton, C. C., and Snyderman, R. (1985) Activation of the respiratory burst enzyme from human neutrophils in a cell-free system. Evidence for a soluble cofactor. *J. Clin. Invest.* **75,** 1735–1739
30. Curnutte, J. T. (1985) Activation of human neutrophil nicotinamide adenine dinucleotide phosphate, reduced (triphosphopyridine nucleotide, reduced) oxidase by arachidonic acid in a cell-free system. *J. Clin. Invest.* **75,** 1740–1743
31. Pick, E., Bromberg, Y., Shpungin, S., and Gadba, R. (1987) Activation of the superoxide forming NADPH oxidase in a cell-free system by sodium dodecyl sulfate. Characterization of the membrane-associated component. *J. Biol. Chem.* **262,** 16476–16483
32. Miller, F. J., Jr., Chu, X., Stanic, B., Tian, X., Sharma, R. V., Davisson, R. L., and Lamb, F. S. (2010) A differential role for endocytosis in receptor-mediated activation of Nox1. *Antioxid. Redox Signal.* **12,** 583–593
33. Lassègue, B., and Griendling, K. K. (2010) NADPH oxidases. Functions and pathologies in the vasculature. *Arterioscler. Thromb. Vasc. Biol.* **30,** 653–661
34. Anderson, K. E., Chessa, T. A., Davidson, K., Henderson, R. B., Walker, S., Tolmachova, T., Grys, K., Rausch, O., Seabra, M. C., Tybulewicz, V. L., Stephens, L. R., and Hawkins, P. T. (2010) PtdIns3P and Rac direct the assembly of the NADPH oxidase on a novel, pre-phagosomal compartment during FcR-mediated phagocytosis in primary mouse neutrophils. *Blood* **116,** 4978–4989
35. El-Benna, J., Dang, P. M., and Gougerot-Pocidalo, M. A. (2008) Priming of the neutrophil NADPH oxidase activation. Role of $p47^{phox}$ phosphorylation and NOX2 mobilization to the plasma membrane. *Semin. Immunopathol.* **30,** 279–289
36. Dewas, C., Dang, P. M., Gougerot-Pocidalo, M. A., and El-Benna, J. (2003) TNF-α induces phosphorylation of $p47^{phox}$ in human neutrophils. Partial phosphorylation of $p47^{phox}$ is a common event of priming of human neutrophils by TNF-α and granulocyte-macrophage colony-stimulating factor. *J. Immunol.* **171,** 4392–4398
37. Dang, P. M., Stensballe, A., Boussetta, T., Raad, H., Dewas, C., Kroviarski, Y., Hayem, G., Jensen, O. N., Gougerot-Pocidalo, M. A., and El-Benna, J. (2006) A specific $p47^{phox}$ serine phosphorylated by convergent MAPKs mediates neutrophil NADPH oxidase priming at inflammatory sites. *J. Clin. Invest.* **116,** 2033–2043
38. DeLeo, F. R., Renee, J., McCormick, S., Nakamura, M., Apicella, M., Weiss, J. P., and Nauseef, W. M. (1998) Neutrophils exposed to bacterial lipopolysaccharide upregulate NADPH oxidase assembly. *J. Clin. Invest.* **101,** 455–463
39. Mansfield, P. J., Hinkovska-Galcheva, V., Shayman, J. A., and Boxer, L. A. (2002) Granulocyte colony-stimulating factor primes NADPH oxidase in neutrophils through translocation of cytochrome b_{558} by gelatinase-granule release. *J. Lab. Clin. Med.* **140,** 9–16
40. Saitoh, S. (2009) Chaperones and transport proteins regulate TLR4 trafficking and activation. *Immunobiology* **214,** 594–600
41. Husebye, H., Halaas, Ø., Stenmark, H., Tunheim, G., Sandanger, Ø., Bogen, B., Brech, A., Latz, E., and Espevik, T. (2006) Endocytic pathways regulate Toll-like receptor 4 signaling and link innate and adaptive immunity. *EMBO J.* **25,** 683–692
42. Bruscia, E. M., Zhang, P. X., Satoh, A., Caputo, C., Medzhitov, R., Shenoy, A., Egan, M. E., and Krause, D. S. (2011) Abnormal trafficking and degradation of TLR4 underlie the elevated inflammatory response in cystic fibrosis. *J. Immunol.* **186,** 6990–6998
43. McGettrick, A. F., and O'Neill, L. A. (2010) Localisation and trafficking of Toll-like receptors. An important mode of regulation. *Curr. Opin. Immunol.* **22,** 20–27
44. Tamassia, N., Le Moigne, V., Calzetti, F., Donini, M., Gasperini, S., Ear, T., Cloutier, A., Martinez, F. O., Fabbri, M., Locati, M., Mantovani, A., McDonald, P. P., and Cassatella, M. A. (2007) The MyD88-independent pathway is not mobilized in human neutrophils stimulated via TLR4. *J. Immunol.* **178,** 7344–7356
45. Inaba, M., Takahashi, T., Kumeda, Y., Kato, T., Hato, F., Yutani, Y., Goto, H., Nishizawa, Y., and Kitagawa, S. (2008) Increased basal phosphorylation of mitogen-activated protein kinases and reduced responsiveness to inflammatory cytokines in neutrophils from patients with rheumatoid arthritis. *Clin. Exp. Rheumatol.* **26,** 52–60
46. Sela, S., Shurtz-Swirski, R., Cohen-Mazor, M., Mazor, R., Chezar, J., Shapiro, G., Hassan, K., Shkolnik, G., Geron, R., and Kristal, B. (2005) Primed peripheral polymorphonuclear leukocyte. A culprit underlying chronic low-grade inflammation and systemic oxidative stress in chronic kidney disease. *J. Am. Soc. Nephrol.* **16,** 2431–2438
47. Suematsu, M., Suzuki, M., Kitahora, T., Miura, S., Suzuki, K., Hibi, T., Watanabe, M., Nagata, H., Asakura, H., and Tsuchiya, M. (1987) Increased respiratory burst of leukocytes in inflammatory bowel diseases. The analysis of free radical generation by using chemiluminescence probe. *J. Clin. Lab. Immunol.* **24,** 125–128